REALISTIC SIMULATIONS OF EXTREME LOAD CASES WITH LIDAR-BASED FEEDFORWARD CONTROL

Tim Hagemann, Florian Haizmann, David Schlipf, Po Wen Cheng

Stuttgart Wind Energy (SWE), University of Stuttgart, Germany, hagemann@ifb.uni-stuttgart.de

Summary

This work presents the development of a simulation environment which allows to simulate realistic extreme events with lidar-based feedforward control. This environment includes turbulent wind fields including extreme events, wind evolution and wind field scanning with a nacelle-based lidar system. It is designed to simulate lidar-based controllers in a realistic environment. In addition, a controller extension is proposed to identify and mitigate extreme events in wind fields based on lidar measurements. The combination of this extreme event controller with the realistic simulation environment is a promising tool for load reductions in wind turbines.

1. Introduction

The design process of wind turbines relies heavily on standardised test environments to determine the structural loads. These environments include turbulent wind fields to assess fatigue loading and specific prescribed events to account for extreme loads.

At the same time, the development of wind turbine control algorithms based on lidar measurements in wind turbine inflow advances, yielding promising results in terms of load reductions. These measurements enable the controller to preview changes in the incoming wind and to adjust the reactions of the turbine. Apart from individual field testing campaigns, the benefits of lidar-based feedforward control have to be demonstrated through simulations. Extreme load cases have proven a popular method in demonstrating these benefits and it is furthermore conceivable to rate the performance of different algorithms with similar standardised simulations. The transferability of these simulation results to a real-life context relies heavily on the assumptions made by the simulation environment. This work provides a step towards this goal by developing a simulation environment which enables to simulate the DTU 10 MW reference wind turbine in extreme operating gusts (EOG) or extreme wind shears (EWS, DLC 1.5) in a more realistic way.

Section 2 of this paper describes the single aspects of the simulation environment. Section 3 presents the controller extension to identify and mitigate extreme events. The results of a simulation of an extreme event are shown and Section 4 gives a conclusion to this paper.

2. Development of a Realistic Simulation Environment

There are two commonly used simplifications for extreme load simulations with lidar-assisted control which are approached in this work:

1. The assumption of coherent wind fields, which means, that the time series of every wind field grid point follows exactly the definition of the event as specified in the IEC standard. Obviously, this approach results in unrealistic wind conditions. A wind field can be considered realistic, if it complies with the requirements of coherence between spatially separated points as defined in the used turbulence model. Realistic wind fields are especially important for simulations with lidar-based control, where the role of measurements in the wind field is as important as the impact of the wind field on the turbine. A coherent wind field makes the task of estimating the rotor-effective wind speed v_0 unrealistically easy, considering that a simple staring scan would result in a perfect lidar estimation of the rotor-effective wind speed $v_{0,\mathrm{L}}$.

2. The assumption of Taylor's frozen turbulence hypothesis [1], which postulates that turbulence eddies convect unchanged with the mean wind speed. In the application of nacelle-based lidar measurements this would imply, that a gust measured by the lidar in the inflow would arrive unchanged at the turbine. The current practice in wind turbine simulations is to assume Taylor's hypothesis but apply a low-pass filter to the lidar measurements to diminish the higher frequencies of the inflow measurements which are more likely to change between the lidar measurement and the impact on the turbine.

The following sections show how these issues are addressed in this work.

2.1. Generation of Turbulent Extreme Event Wind Fields

The wind field generation and the lidar-based controller in this work uses the least-squares wind field reconstruction. Hence, this method is presented in advance:
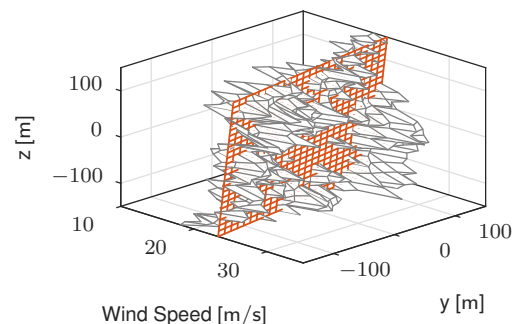

Figure 1: The longitudinal wind component of a wind field (grey) for one point in time with the respective least-squares plane (red) calculated with Equation 1.

The least-squares wind field reconstruction method is able to estimate the shear of the incoming wind field from lidar measurements. This method assumes the incoming
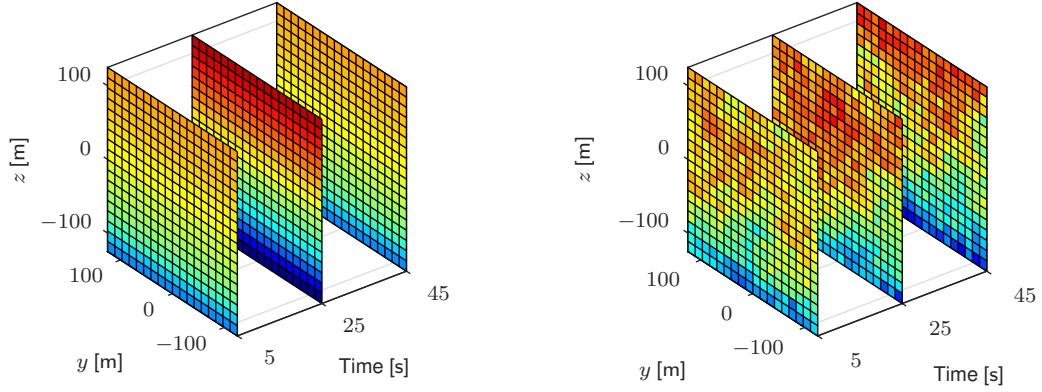
Figure 2: Conventional wind field for EOG simulations (left) and turbulent EOG wind field produced in this work(right).

wind as a plane with v_0 as the mean wind speed and a horizontal and vertical gradient δ_H and δ_V. Figure 1 depicts the relation between the least-squares plane and the longitudinal wind speeds in the wind field. The wind field characteristics are computed by solving the following system of equations:

$$
\begin{pmatrix} x_{L,1} & x_{L,1}y_{L,1} & x_{L,1}z_{L,1} \\ x_{L,2} & x_{L,2}y_{L,2} & x_{L,2}z_{L,2} \\ \vdots & \vdots & \vdots \\ x_{L,n} & x_{L,n}y_{L,n} & x_{L,n}z_{L,n} \end{pmatrix} \begin{pmatrix} v_{0,L} \\ \delta_{H,L} \\ \delta_{V,L} \end{pmatrix} = \begin{pmatrix} f_1 v_{los,1} \\ f_2 v_{los,2} \\ \vdots \\ f_n v_{los,n} \end{pmatrix},
$$

(1)

with the coordinates $x_{L,n}, y_{L,n}, z_{L,n}$, the focus length f_n and the measured line-of-sight wind speed $v_{los,n}$ of a measurement point n. The background of this wind field reconstruction method is discussed more extensively in [2]. The advantage of this method is the estimation of linear horizontal and vertical shear via the plane's gradients δ_H and δ_V.

This work uses a tool as developed in [3] to create realistic wind fields. This tool creates a turbulent wind field to a predefined characteristic by setting up a cost-function which defines specific values over time, which should be matched by the resulting wind field. The tool then runs an optimisation algorithm and fits the wind field to the requested characteristics.

The original tool is designed to create wind fields containing an extreme operating gust. In this work, the wind field generation tool is extended to generate a wind field which inherits an extreme wind shear event. For this purpose, a reference behaviour over time is defined for the rotor-effective wind speed v_0, the linear vertical shear δ_V and the linear horizontal shear δ_H. The optimisation process is set up to minimise the following vector cost function:

$$
\begin{pmatrix} v_{0,ref} \\ \delta_{V,ref} \\ \delta_{H,ref} \end{pmatrix} - \begin{pmatrix} v_{0,simulated} \\ \delta_{V,simulated} \\ \delta_{H,simulated} \end{pmatrix}.
$$

(2)

The reference values $v_{0,ref}$, $\delta_{V,ref}$ and $\delta_{H,ref}$ are determined by creating a coherent wind field according to the EWS event as defined in the standard and applying the least-squares wind field reconstruction method as shown

above. In each step in the optimisation process, this reconstruction method is carried out to retrieve the values for $v_{0,simulated}$, $\delta_{V,simulated}$ and $\delta_{H,simulated}$. The cost function then calculates the residual which is minimised by the optimiser.

Figure 2 shows the difference between the conventional coherent wind field and the more realistic wind field for an EOG. The improvement towards realistic wind fields is clearly visible as the wind field contains the extreme operating gust as seen by the rotor but is still a turbulent wind field.

2.2. Wind Evolution

There are two wind evolution models which can be implemented in the aero-elastic simulation software DNV GL Bladed:

- Exponential model
- Kristensen model

To describe the decay of the wind field, both models define the coherence between wind speeds at two points on a longitudinal distance. The coherence assigns a rate of decay to every frequency in the wind field on this distance. In the case of Taylor's frozen turbulence, the coherence would be unity on all frequencies, as the signals would be perfectly correlated. This work only uses the Exponential model due to its simplicity.

The Exponential model has been defined in [4] and is based on wind measurements with cup anemometers. It states, that the coherence between two met mast wind measurements falls off exponentially, which leads to the definition of the coherence:

$$
\gamma^2(k) = \exp(-\alpha k \Delta x),
$$

(3)

with the exponential decay factor α, a downstream distance Δx, the wave number $k = \frac{2\pi f}{\overline{v}}$ and the mean wind speed $\overline{v}$. In this work α is chosen to a value of 0.3 based on field testing results [5].

The method of modelling evolving turbulence in Bladed is described in [6]: Two 3D turbulent wind fields have to be created, which are identical except for their random seed. Wind field 1 impacts the turbine throughout the entire simulation, while wind field 2 is present at an infinitive upwind distance from the turbine. If a lidar measurement

2

is carried out in front of the turbine, the measured time series is computed by

$$u(t) = \sum_{i=1}^{N} S_u(f_i) \cos(2\pi f_i t + d_i \phi_{i,1} + (1-d_i)\phi_{i,2}), \quad (4)$$

with the spectrum of the wind speed in u-direction S_u, the frequencies f_i and the phases for each wind field and frequency $\phi_{i,1}$ and $\phi_{i,2}$ as well as the decay fraction d_i:

$$d_i = \sqrt{\gamma^2(f_i)}, \quad (5)$$

using the coherence function $\gamma^2(f_i)$ of the selected wind evolution model and measurement distance.

2.3. Lidar Simulation

Since Version 4.5, Bladed is able to model a nacelle-based lidar measurement in wind turbine simulations with variable scan patterns. For this work, the scan patterns are designed using an optimisation algorithm developed in [5]. The algorithm alters the shape of circular scans in five measurement planes and optimises the coherence γ_{RL}^2 between v_0 and the lidar-based estimation of the rotor-effective wind speed $v_{0,L}$. For an environment with evolving turbulence, the algorithm leads to a circular pattern with eight measurement points, an opening angle of $31°$ and the five measurement distances $d = [0.3, 0.475, 0.65, 0.825, 1] \cdot D$, with the rotor diameter D. Figure 3 shows the coherence γ_{RL}^2 of v_0 and the lidar-based estimation $v_{0,L}$ with and without wind evolution. It is visible, that the optimised scan pattern results in the expected coherence characteristic as it coincides with the expected γ_{RL}^2 from the pattern optimisation algorithm.
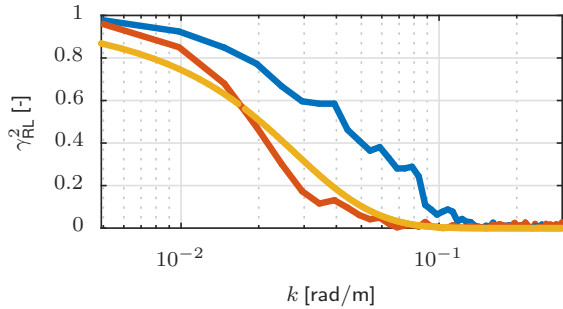

Figure 3: Coherence characteristic of optimised scan pattern in simulation with (red) and without wind evolution (blue) as well as the expected coherence from the scan pattern optimisation (yellow).

3. Lidar-Based Controller

The controller used in this work consists of a baseline feedback controller combined with a lidar-assisted feedforward controller which adjusts the pitch rate of the turbine and has been developed in [7]. The controller is extended with an algorithm which detects extreme events (such as EOG and EWS) based on lidar measurements and puts the turbine into a *safety mode* by reducing the generator speed Ω_G.

The algorithm is designed to identify events which are similar to extreme events as defined in the standard. For this purpose, the maximum gradient of the v_0 signal $\max(\frac{\Delta v_0}{\Delta t})$ is computed with a tunable parameter Δt set to the rising time of a standard gust. At the same time, the maximum and minimum of the least-squares linear shear values δ_V and δ_H are retrieved from the lidar measurements. As a result five diagnostic parameters are checked against a threshold to identify an extreme event:

$$\max\left(\frac{\Delta v_0}{\Delta t}\right) \geq \dot{v}_{\max} \quad (6)$$

$$\max(\delta_V) \geq \delta_{V,\max} \quad (7)$$

$$\min(\delta_V) \leq \delta_{V,\min} \quad (8)$$

$$\max(\delta_H) \geq \delta_{H,\max} \quad (9)$$
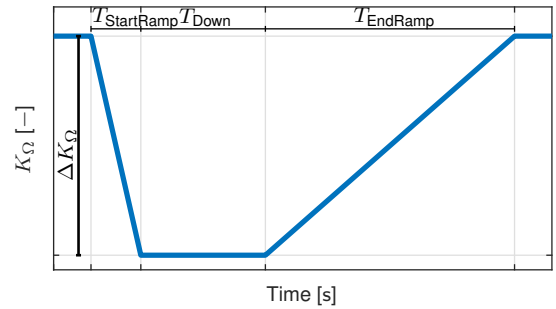
$$\min(\delta_H) \leq \delta_{H,\min} \quad (10)$$

Figure 4: Safety mode ramping sequence of K_Ω.

To identify the EOG, the gradient $\frac{\Delta v_0}{\Delta t}$ is chosen, while the absolute values for δ_H and δ_V are used to identify the EWS. After a check if the trigger was a single outlier, the safety mode is activated.

The safety mode consists of a ramping sequence in the reference signal of the feedback pitch controller. To allow for a safety mode, the reference signal of the feedback pitch controller equals the rated generator speed $\Omega_{G,rated}$ multiplied by a factor K_Ω:

$$\Omega_{G,ref} = K_\Omega \cdot \Omega_{G,rated}. \quad (11)$$

If the safety mode is triggered, K_Ω follows a ramping sequence, which is shown in Figure 4, resulting in a transiently reduced generator speed. The ramping sequence is fully tunable by the four parameters $T_{StartRamp}, T_{Down}, T_{EndRamp}$ and ΔK_Ω.

A decrease in the reference generator speed results in lower aerodynamic power and protects the wind turbine from higher loads and possible emergency shutdowns.

4. Results

In the case of an extreme operating gust, the safety mode is built to prevent an emergency stop caused by a rotor overspeed alert.

Figure 5 shows the v_0 characteristic of an EOG and the wind turbine's reaction to it. The simulations are carried out with a feedback controller and a lidar-based feedforward controller with extreme event identification. For the
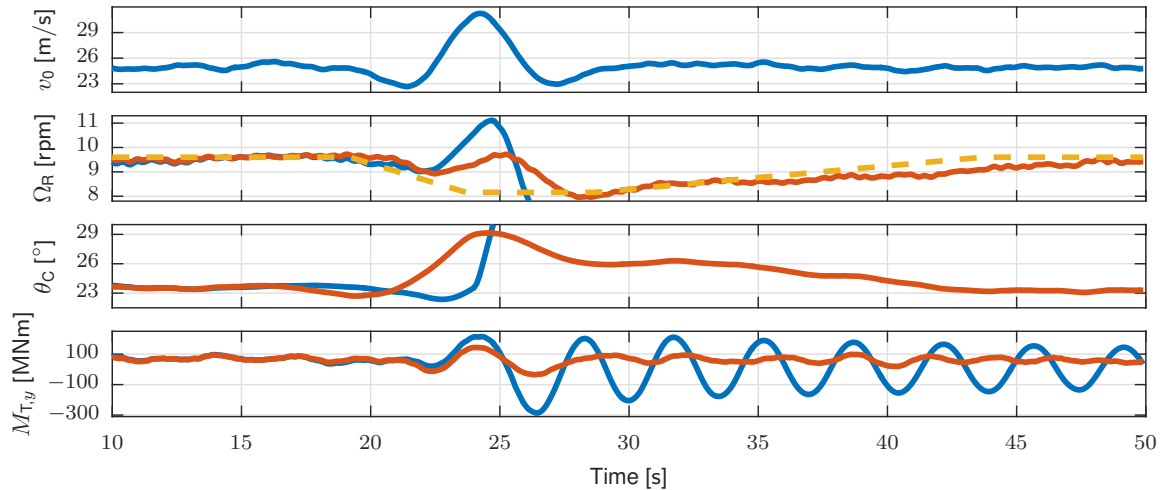
Figure 5: Simulation results of an EOG simulation with a feedback controller (blue), a feedforward controller with extreme event identification (red) as well as the safety mode characteristics (yellow). The feedback controller produces an overspeed alert and triggers an emergency stop at $t = 24\,\text{s}$.

feedback controller, the EOG results in an emergency shutdown caused by an overspeed alert at $t = 24\,\text{s}$. The activated safety mode as indicated by the dashed yellow line, leads to an earlier pitching and ultimately prevents an emergency shut down for the simulation with the controller extension of this work. In consequence higher loads such as the substantial oscillations, which are observable in the tower base bending moment $M_{\text{T},y}$, are avoided. The maximum rotor speed is reduced by $8\,\%$ and the maximum absolute value of the tower base bending moment $M_{\text{T},y}$ is reduced by $50\,\%$.

5. Conclusion

This work presents an extension to the engineering approach to shape realistic wind fields to extreme operating gusts. This extension allows the generation of realistic wind fields containing an extreme wind shear event by defining a vectorised cost-function to the optimising algorithm. These realistic wind fields are used in a simulation environment allowing to simulate extreme events with wind evolution and optimised scan patterns for lidar-based feedforward control.

In a second step, the feedforward controller is extended to identify extreme events based on simulated lidar measurements. A simple safety mode is proposed to avoid higher loads on the wind turbine.

Based on this work, more advanced extreme event mitigation techniques can be developed, e.g. an individual pitch approach as presented in [8] as well as flatness-based controller approaches. A possible improvement to the extreme event identification is to introduce thresholds dependent on the mean wind speed.

Acknowledgements

References

[1] Taylor, G. I., "The Spectrum of Turbulence," *Proceedings of the Royal Society of London*, Vol. 164 of *A, Mathemathical an Physical Sciences*, The Royal Society, 1938, pp. 476–490.

[2] Haizmann, F., Schlipf, D., and Cheng, P. W., "Correlation-model of rotor-effective wind shears and wind speed for lidar-based individual pitch control," *DEWEK*, Bremen, 2015.

[3] Schlipf, D. and Raach, S., "Turbulent Extreme Event Simulations for Lidar-Assisted Wind Turbine Control," *TORQUE*, Munich, 2016, Journal of Physics: Conference Series.

[4] Pielke, R. A. and Panofsky, H. A., "Turbulence characteristics along several towers," *Boundary-Layer Meteorology*, Vol. 1, No. 2, 1970, pp. 115–130.

[5] Schlipf, D., Haizmann, F., Cosack, N., Siebers, T., and Cheng, P. W., "Detection of wind evolution and lidar trajectory optimization for lidar-assisted wind turbine control," *Meteorologische Zeitschrift*, Vol. 24, 2015, pp. 565–579.

[6] Bossanyi, E., "Un-freezing the turbulence: improved wind field modelling for investigating Lidar-assisted wind turbine control," *Proceedings of the European Wind Energy Association annual event*, Copenhagen, Denmark, 2012.

[7] Schlipf, D., *Lidar-Assisted Control Concepts for Wind Turbines*, Ph.D. thesis, University of Stuttgart, 2016.

[8] Haizmann, F., Hagemann, T., Schlipf, D., and Cheng, P. W., "Realistic extreme event simulation of lidar-assisted individual pitch control," *presented at WESC*, Copenhagen, 2017.